KSME Journal, Vol. 8, No. 2, pp. 107~114, 1994 

# Analysis of 3D Shape and Strain Distributions of a Deformable Object Using Stereo Vision

**I. H. Yang***

(*Received December 1, 1992*)

This paper proposes a method for analyzing three-dimensional shape and strain distributions of a deformable object using stereo vision. The three-dimensional coordinates of the surface points of an object have been calculated using stereoscopic method. The Fourier transform grid method is applied to high-precision 3D shape and strain distribution of deformable objects by analyzing the phase distribution of grating images. In the conventional automated grid method, because the position of a grid point is expressed by an integer number of pixels, it is difficult to obtain accurate measurement. Using two-dimensional Fourier transform grid method and a two-dimensional cross grating on the surface of the object, we can easily and accrately find the correspondence using phase information and seperate each directional grating line from the two-dimensional grating. Applications for analyzing shape and strain distributions of deformable objects are shown.

**Key Words:** Image Processing, Stereo Vision, Shape Measurement, Strain Analysis, Fourier Transform Grid Method.

## 1. Introduction

The analysis of shape and strain distribution is very important for optimum design. It is especially difficult to measure them of a deformable object or a vibrating object using contact methods, because it is labor intensive, time-consuming and expensive in data collection and analysis. Some grating methods using image processing have been proposed to measure shape or strain of objects. Sciammarella and Sturgeon(1967) have developed a method for analyzing the phases of mismatched fringes by using one-dimensional Fourier transform. Takeda and Mutoh(1984) presented Fourier transform profilometry for measuring the shape of an object. This method analyzed the shape using phase information of a projected grating on the surface of the object. Although it can measure the shape. it cannot measure the strain distributions on the surface of the object. Morimoto et al.(1988, 1990) have developed a new method to analyze strain distribution by using one harmonic of the Fourier spectra of the image of a deformed grating. Moreover, we have previously proposed the Fourier transform grid method to measure the three-dimensional shape and strain distributions of vibrating objects by analyzing the two-dimensional grating images recorded with two cameras. In order to measure the shape and strain distributions of a deformable object, some marks should be put on the surface of the object. The automated Fourier transform grid method is extended to measure them of a deformable object by combining with a stereo vision.

The stereo vision requires to find the points on the images corresponding to the points on the surface of the object. The coordinates of each point on the surface of the object are measured using the corresponding images. Chao et al. (1989) found that camera calibration can affect the strain accuracy of stereo digital correlation method. A grid, or any scene for that matter,

*Department of Ocean Environmental Engineering, Cheju National University, 1 Ara Dong, Cheju, 690-756, Korea

experiences a series of transformations before it is finally stored in the computer's memory as a digital image. The most common types transformations include coordinate translation and rotation, lens distortion, perspective transformation, and CCD image stretching. A general pinhole camera calibration which includes all of the above transformations will be developed, and the relevance of each transformation assessed. In order to obtain accurate results, it is important to measure the parameters of the system such as camera positions and directions.

In order to determine the parameters of the system accurately and easily, a method has been proposed using standard gratings drawn on flat plates and the Fourier transform grid method, and a vibrating object has been analyzed by Yang et al(1992). The accuracy is no good, and it takes much time to adjust and measure the camera positions.

Therefore, we analyze the three-dimensional shape and the strain distributions of a deformable objcet by using this Fourier transform grid method. The Fourier transform grid method can be automated by taking advantage of solid state video technology and pattern recognition algorithms. The potential advantages of automated Fourier transform grid method over conventional grid method are increased speed and accuracy. The primary advantages of automated Fourier transform grid method enjoy over the techniques which are traditionally recognized as more accurate is that specialized training is not needed to interpret the grid method results, and that no additional effort is required for analysis of the three-dimensional shape and the strain distributions. A two-dimensional cross grating recorded by cameras is easily separated into each directional grating and the brightness phases in each direction are calculated using Fourier transform grid method. Using the phase information, the correspondence between the surface point of an object and the points on the images can be performed easily and fast. We show the details of the analysis procedures in this paper and measure the three-dimensional shape and the strain distributions when the pressure of tire increases.

## 2. Principles of Measurement

### 2.1 Calculation of 3D coordinates by stereo vision

The stereo vision is a method to measure the three-dimensional coordinates on the surface of an object from the geometric relationship between two cameras and two images of the object recorded from different directions with two CCD cameras. Figure 1 shows the geometrical relation between the two cameras and the object. As all of the lines from points on the object to the image plane pass through the center point of the camera lens, the coordinates of a point on the image plane determine one of such lines in the three-dimensional space. The point P is on the object and the points $L_1$ and $L_2$ are the centers of the lenses of the cameras respectively. $l_1$ and $l_2$ are the lines connecting from the point P to the points $L_1$ and $L_2$ respectively.

Now the point P projects to the points $S_1$ and $S_2$ on the image planes 1 and 2 respectively. The line connecting between the points $S_1$ and $L_1$ and the line connecting between the points $S_2$ and $L_2$ are determined as $\vec{u_1}=\overrightarrow{S_1L_1}$ and $\vec{u_2}=\overrightarrow{S_2L_2}$ respectively. The three-dimensional coordinates of the points $S_1$ and $S_2$ are calculated from the two-dimensional coordinates on the image planes using the parameters of the cameras. The position vectors of points $L_1$ and $L_2$ are determined as $\vec{a_1} = \overrightarrow{O_1L_1}$ and $\vec{a_2} = \overrightarrow{O_2L_2}$ respectively. As both

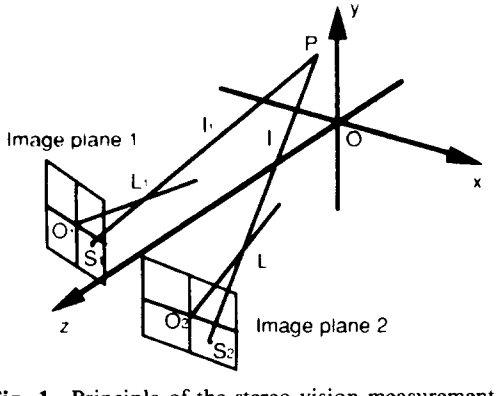


**Fig. 1** Principle of the stereo vision measurement

lines $l_1$ and $l_2$ are the lines from the point P, the coordinates of the point P can be calculated as the intersection of the lines $l_1$ and $l_2$. However in practice, two lines in the space may not have an intersection because of the measurement error. The center point of the common normal segment of the tow lines is adopted instead of the intersection. When the points G and H are on $\overrightarrow{S_1L_1}$ and $\overrightarrow{S_2L_2}$ respectively, the position vectors of points G and H are expressed as follows.

$$\begin{aligned}\overrightarrow{O_1G} &= \overrightarrow{a_1} + t_1\overrightarrow{u_1},\\ \overrightarrow{O_2H} &= \overrightarrow{a_2} + t_2\overrightarrow{u_2}\end{aligned} \tag{1}$$

Where $t_1$ and $t_2$ are factors which determine the points G and H.

The points G and H are determined as $|\overrightarrow{GH}|$ becomes minimum, that is, $\overrightarrow{GH}$ are normal to both of $\overrightarrow{u_1}$ and $\overrightarrow{u_2}$. Then the points G and H can be expressed as

$$\begin{aligned}\overrightarrow{GH}\cdot\overrightarrow{u_1} &= \{(\overrightarrow{a_2} + t_2\overrightarrow{u_2}) - (\overrightarrow{a_1} + t_1\overrightarrow{u_1})\}\cdot\overrightarrow{u_1} = 0,\\ \overrightarrow{GH}\cdot\overrightarrow{u_2} &= \{(\overrightarrow{a_2} + t_2\overrightarrow{u_2}) - (\overrightarrow{a_1} + t_1\overrightarrow{u_1})\}\cdot\overrightarrow{u_2} = 0.\end{aligned} \tag{2}$$

The factors $t_1$ and $t_2$ are obtained by solving these simultaneous equations. $\overrightarrow{O_1G}$ and $\overrightarrow{O_2H}$ can be calculated using these factors and Eq. (1). As mentioned previously, the three-dimensional coordinates of a point on the surface of an object are obtained as the intersection of two lines passing through each lens and a pixel point of each image. The point P which is the middle point of the points G and H can be calculated using the following equation.

$$\overrightarrow{OP} = (\overrightarrow{O_1G} + \overrightarrow{O_2H})/2 \tag{3}$$

### 2.2 Calculation of surface strain distribution

Surface strains are calculated from the three-dimensional coordinates of the grating points on the surface of the object before and after deformation. Figure 2 shows the schemes of the surface of a object before and after deformation. The three-dimensional coordinates of the points C, A and B on the surface are calculated by the stereo vision. After deformation, the points C, A and B move to the points C′, A′ and B′ respectively. $\overrightarrow{x}$ and $\overrightarrow{y}$ are the unit vectors on the plane which is made by the three points C, A and B and they are perpendicular to the y and x axis respectively. The point

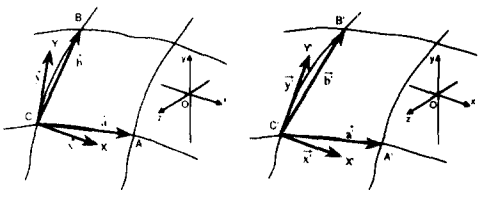

(a) Before deformation (b) After deformation

**Fig. 2** Schemes of surface of object before and after deformation

C is the commom start point and the points X and Y are the end points of $\overrightarrow{x}$ and $\overrightarrow{y}$ respectively. The vectors $\overrightarrow{a}$, $\overrightarrow{b}$, $\overrightarrow{a'}$ and $\overrightarrow{b'}$ are defined as follows.

$$\begin{aligned}\overrightarrow{a} &= \overrightarrow{CA},\\ \overrightarrow{b} &= \overrightarrow{CB},\\ \overrightarrow{a'} &= \overrightarrow{C'A'},\\ \overrightarrow{b'} &= \overrightarrow{C'B'}\end{aligned} \tag{4}$$

As $\overrightarrow{a}$ and $\overrightarrow{b}$ are the linearly independent, the unit vectors $\overrightarrow{x}$ and $\overrightarrow{y}$ can be expressed with factors $p$, $q$, $r$ and $s$ as follows.

$$\begin{aligned}\overrightarrow{x} &= p\overrightarrow{a} + q\overrightarrow{b},\\ \overrightarrow{y} &= r\overrightarrow{a} + s\overrightarrow{b}\end{aligned} \tag{5}$$

$\overrightarrow{x'}$ and $\overrightarrow{y'}$ are determined with these factors $p$, $q$, $r$ and $s$ as follows.

$$\begin{aligned}\overrightarrow{x'} &= p\overrightarrow{a'} + q\overrightarrow{b'},\\ \overrightarrow{y'} &= r\overrightarrow{a'} + s\overrightarrow{b'}\end{aligned} \tag{6}$$

When the points X′ and Y′ are defined as the end points of $\overrightarrow{x'}$ and $\overrightarrow{y'}$, these points correspond to the points X and U respectively before deformation. The strains of a deformable object are given as

$$\begin{aligned}\varepsilon_x &= \frac{|\overrightarrow{x'}| - |\overrightarrow{y}|}{x},\\ \varepsilon_y &= \frac{|\overrightarrow{y'}| - |\overrightarrow{y}|}{y},\\ \tau &= \frac{\pi/2}{arg(\overrightarrow{x}, \overrightarrow{y})}\{arg(\overrightarrow{x}, \overrightarrow{y}) - arg(\overrightarrow{x'}, \overrightarrow{y'})\}\end{aligned} \tag{7}$$

Where $arg(\overrightarrow{x}, \overrightarrow{y})$ means the angle between $\overrightarrow{x}$ and $\overrightarrow{y}$. By applying these equations to all the points on the whole surface recorded on the images, strain distributions of a deformable object are obtained.

## 3. Theory of Fourier Transform Grid Method

In the conventional grid method using an image processing technique, the position of a grid line is measured by an integer number of pixels. The Fourier transform grid method is introduced here for obtaining the position in a decimal unit and for finding the corresponding points between different images of the same grating. In order to analyze a two-dimensional grid image, a cross grating with orthogonal linls as shown in Fig. 3 is employed. The brightness intensity function of the cross grating can be expressed as the product of two single grating intensity functions. One single grating normal to the x axis denoted as the x grating, and another single grating normal to the y axis denoted as the y grating, are utilized for strain measurements in the x and y directions respectively. The expansion of the intensity function of the cross grating g(x, y) in Fourier series is

$$g(x, y)=\sum_{m=-\infty}^{\infty}\sum_{n=-\infty}^{\infty} i_{m,n}(x, y) \exp\{j2\pi m\omega_x x+j2\pi n\omega_y y\} \quad (8)$$

Where $i_{m,n}$ is the coefficient of the harmonic of the order(m, n), m and n are integers, $j$ is the imaginary unit, and $\omega_x$ and $\omega_y$ are frequencies of the x and y gratings respectively. The Fourier transform of g(x, y) is expressed by

$$G(\Omega_x, \Omega_y)=\int_{-\infty}^{\infty}\int_{-\infty}^{\infty} g(x, y) \exp\{-j2\pi(\Omega_x x+\Omega_y y)\}dx dy = \sum_{m=-\infty}^{\infty}\sum_{n=-\infty}^{\infty} I_{m,n}(\Omega_x-m\omega_x, \Omega_y-n\omega_y) \quad (9)$$

where $I_{m,n}(\Omega_x, \Omega_y)$ is the Fourier transform of $i_{m,n}$ (x, y). $\Omega_x$ and $\Omega_y$ are the x and y directional frequencies respectively. Figure 4 shows a schema of the two dimensional Fourier spectrum of the grating. Each circle shows the region where the harmonic of the order(m, n) exists. Let us show the analysis in the x direction. The (1, 0) order harmonic indicated with oblique lines in Fig. 4 is extracted by filtering, and its inverse Fourier transform is computed as the following equation.

$$i_{1,0}(x, y)=\int_{-\infty}^{\infty}\int_{-\infty}^{\infty} I_{1,0}(\Omega_x-\omega_x, \Omega_y) \exp\{j2\pi(\Omega_x x+\Omega_y y)\}d\Omega_x d\Omega_y = C_{1,0}\exp\{j\theta_x(x, y)\} \quad (10)$$

The argument of Eq. (10) or the phase of the grating line contains the displacements. These grating lines can also be used as the corresponding points before and after deformation. The real and imaginary parts of Eq. (10) are

$$Re\{i_{1,0}(x, y)\}=C_{1,0}\cos\{\theta_x(x, y)\},$$
$$Im\{i_{1,0}(x, y)\}=C_{1,0}\sin\{\theta_x(x, y)\}. \quad (11)$$

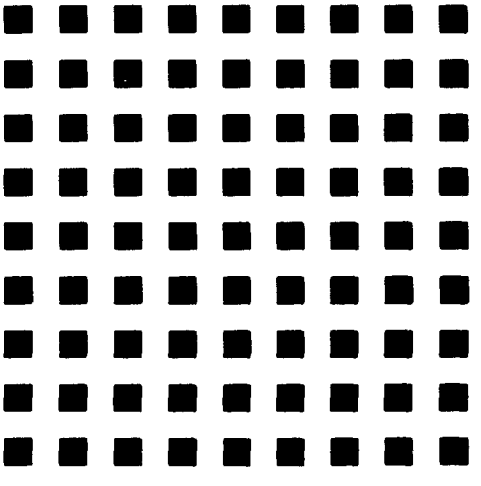

**Fig. 3** Two-dimensional grating image

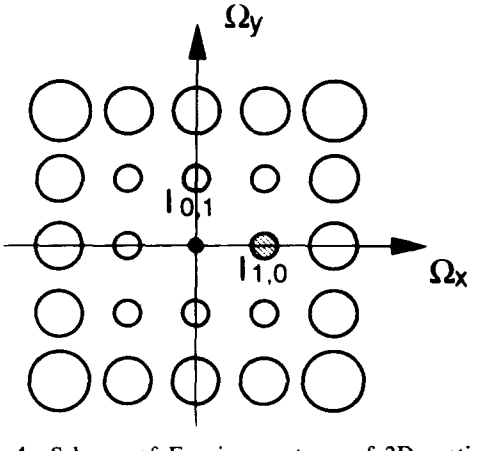


**Fig. 4** Schema of Fourier spectrum of 2D grating image

Each equation shows a sinusoidal fringe pattern. The image of this equation shows only the x grating. The phase distribution $\theta_x(x, y)$ is obtained by calculating

$$\theta_x(x, y) = \arctan \frac{Im\{i_{1,0}(x, y)\}}{Re\{i_{1,0}(x, y)\}}. \quad (12)$$

Similarly, the phase distribution $\theta_y(x, y)$ of the y grating is obtained. The position of the point(x, y) corresponding to a certain phase ($\theta_x$, $\theta_y$) can be calculated in a decimal pixel unit by a two-dimensional interpolation based on the continuity of phase distribution. Since the phases obtained by Eq. (12) are confined to the range of $-\pi$ to $\pi$ the phases are adjusted so as to be continuous by adding or subtracting $2\pi$. Based on the information of a reference line, a phase distribution in each image is calculated. Furthermore, in order to match the corresponding points between different images, a reference point is selected in each image with the same phase value. If two points in the different images have the same phases in both the x and y directions, they are identified as the corresponding points and their matching process can be automatically performed.

## 4. Experimental Results and Discussions

The three-dimensional shape and the strain distributions of the surface of a deformable object are analyzed by the method mentioned above. In order to measure 3D shape and strain distribution of a deformable object, the measurement system shown in Fig. 5 was developed based on the stereoscopic method. A two-dimensional grating pattern with a pitch 2 mm is drawn on the side of a tire before deformation.

During the experiment, the images of the grating on the deformable object are simultaneously recorded with two video cassette recorders. The recorded video images are changed to the digital image using an image grabber. Figure 6 shows the grating image recorded by the left camera when the pressure is 3.0 kg/cm$^2$. The pitch between two grating lines in each image is about 8 pixels. The analyzed region is about 60 mm × 80 mm near the center. The analysis of the shape and the strain distributions is performed when the pressure is 0.0, 1.0, 2.0 and 3.0 kg/cm$^2$. Each image obtained from cameras is transformed to the Fourier spectrum by calculating the Fourier transform. The Fourier spectrum of the grating image is shown in Fig. 7. The cross gratings can

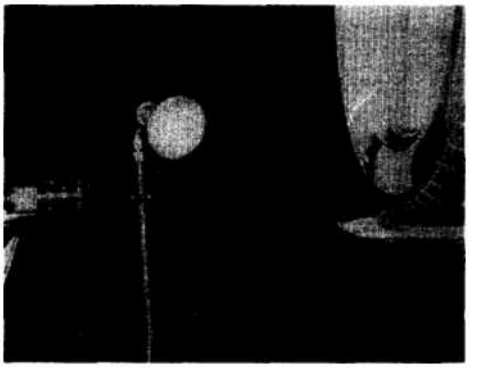

**Fig. 5** Measurement system

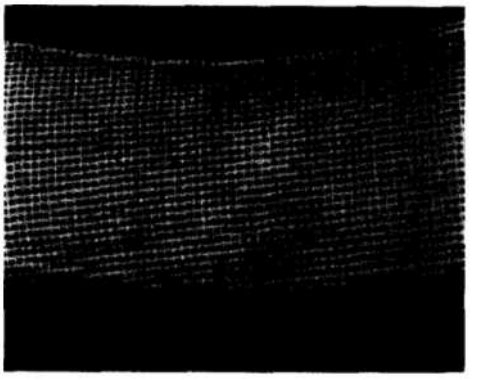

**Fig. 6** Two-dimensional grating image of left camera

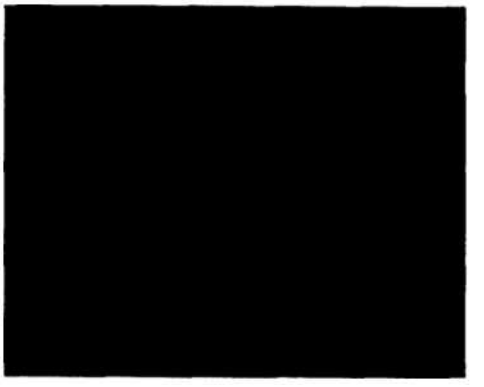

**Fig. 7** Fourier spectrum of 2D grating image

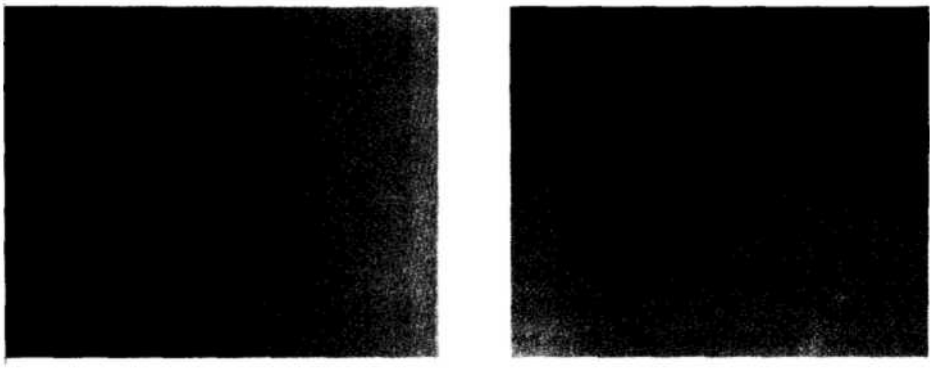

(a) $X$-directional phase distribution (b) $Y$-directional phase distribution

**Fig. 8** Phase distribution of $x$-and $y$-directional first harmonic

be divided to the one-dimensional grating for each x and y direction by extracting the first harmonic of each direction and calculating the inverse Fourier transform. In general, the overlappings between the first harmonic and other harmonics depend on the deformation state or strain distribution. It is evident that the overlapping phenomenon is initiated by the encounter between the highest frequency compoment of the first harmonic and the lowest frequency component of another harmonic of the order. If each of the first harmonics in the x and y directions is not overlapped by other harmonics, it can be extracted respectively. However, if the first harmonic extraction is not complete, some errors occur. The first harmonic of Fourier spectrum of a grating image corresponds to the high brightness intensity component. Because of the phase distribution corresponding to the brightness distrbution and the continuity of the phase distribution, the position of the grating is calculated by a decimal number of pixels by interpolating the corresponding distribution. Figure 8 shows the phase distribution obtained by calculating the inverse Fourier transform of each first harmonic. Every grating line in x and y directions has a line number for each direction.

From the phase of a reference point in each image, the phase distributions in the x and y directions can be calculated. These line numbers increase or decrease monotonically on the surface of the object. As the phase is in proportion to the line number, it can be used for corresponding instead of the line number. Therefore every pixel on the image has a decimal line number obtained from the phase information. By analyzing the phase distribution of the grating, not only the accurate positions of the grating line can be obtained, but the matching of the corresponding grating points in the different images can also be automatically performed.

The phase is obtained by calculating the ratio of the brightness of the imaginary part to that of the real part at each point. From the phase of a reference point in each image, the phase distributions in the x and y directions can be calculated. By analyzing the two-dimensional phase distributions in both the right and left images, the exact positions of the intersection in each image are obtained. The three-dimensional positions of grid points are determined by Eq. (3) The positions of the intersection of the grating are stored in a database. By applying this method to stereoscopic measurement system, the shape of a deformable object can be measured. Figure 9 shows the deformation of the three-dimensional shapes when the pressure increases. After deformation, the shape of the deformable object is measured by the same method, and another three-dimensional shape database is formed by the same corresponding points. Figure 10 shows the comparison of the shape obtained by this proposed method and the shape measured by a dial gauge before deformation. The maximum difference is 0.76 mm and

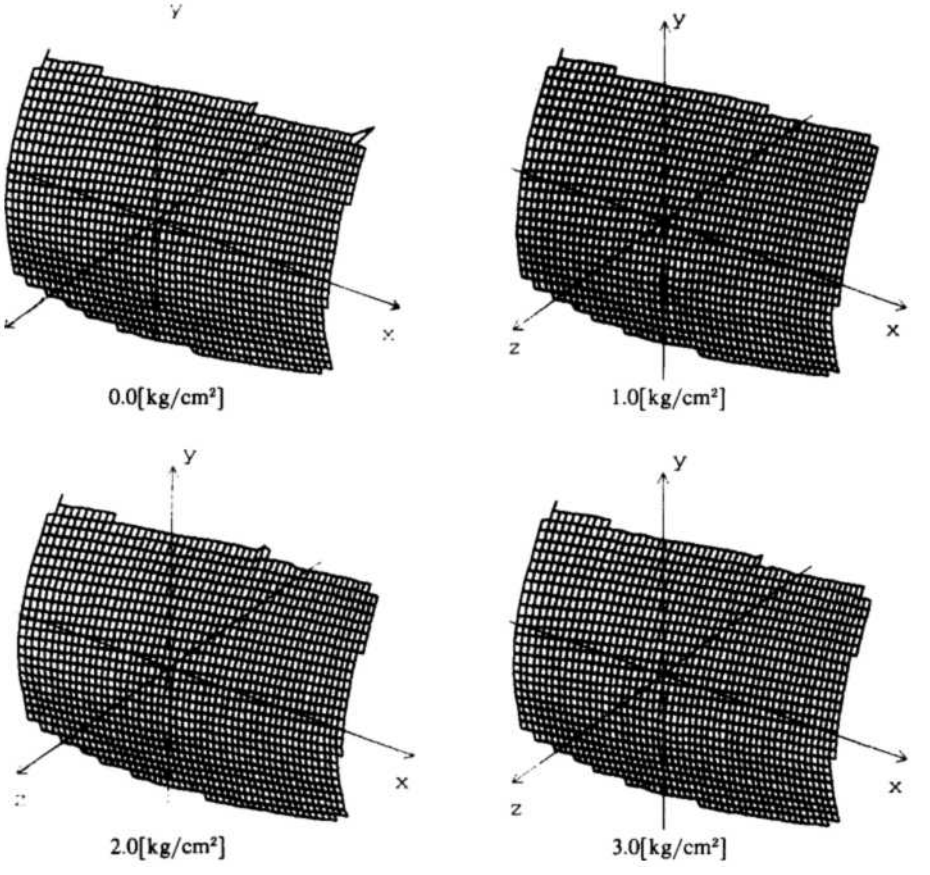


**Fig. 9** Shapes with different pressure

the average of the absolute differences is 0.27 mm. The error may be due to optical distortions, any electrical and mechanical changes, the error of parameter measurement and so on. The argument of Eq. (10) includes the information of the displacement. By substituting the argument $\theta_x(x, y)$ obtained from Eq. (12) into Eq. (10), we can calculate the displacement of the x grating. Similarly, the displacement of the y grating is obtained. Therefore, we are able to obtain the displacement on pixel by pixel because the phase at each pixel point gives the information of the displacement at the point. The surface strain distributions of deformable objects are calculated by differentiating the displacement obtained from the continuous arguments. Figure 11 shows the surface strain distributions with pressure displacement. The distributions of strain were analyzed when the pressure is 0.0, 1.0 and 2.0 kg/cm² respectively. It is noted that the strain near the center of the deformable object becomes larger

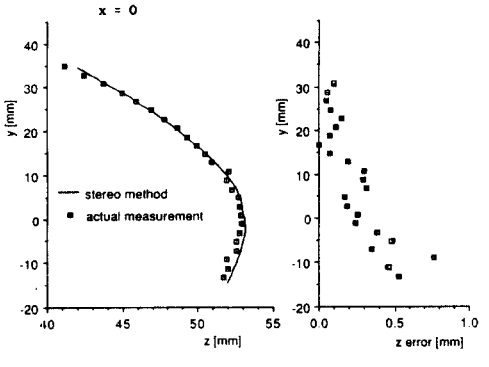


**Fig. 10** Comparison of shape obtained by this proposed method and shape measured by dial gauge before deformation

**Fig. 11** Strain distributions with pressure displacement

with the increasing displacement of the pressure.

## 5. Conclusions

The important features which distinguish the automated Fourier transform grid method described in this paper are simplicity and speed. The simplicity of the algorithm enables full-field strain analysis to be accomplished in under 180 seconds with a personal computer. A two-dimensional cross grating recorded by two cameras is easily seperated into each directional grating and the brightness phases in each direction are calculated using Fourier transform grid method. By analyzing the phase distribution, the correspondence between the surface point of an object and the points on the images can be performed easily and fast. The coordinates of each point on the surface of the object are accurately measured using the corresponding images. The coordinates of all points, which have arbitary phase vectors of grating lines, are obtained in a decimal number of pixels on the image. The three-dimensional shape and strain distributions of a deformable object with the increase of pressure using the stereo vision are measured.

## References

Chao, Y. J., Sutton, M. A., Peters, W. H. and Luo, P. F., 1989, "Measurement of Three-dimensional Displacements and Deformations in Deformable Bodies Image Processing," Proceedings of the SEM Spring Conference of Exp. Mech., pp. 139~146.

Morimoto, Y. and Seguchi, Y., 1988, "Application of Moire Analysis of Strain Using Fourier Transform," Optical Engineering, Vol. 27, No. 8, pp. 650~656.

Morimoto, Y., Seguchi, Y. and Higashi, T., 1990, "Strain Analysis by Moire Method and Grid Method Using Fourier Transform," Comp. Mech., Vol. 6, No. 1, pp. 1~10.

Scimmarella, C. A. and Sturgeon, D. L., 1967, "Digital-filtering Technicques Applied to the Interpolating of Moire-fringes Data," Exp. Mech., Vol 7, No. 11, pp. 468~475.

Takeda, M. and Mutoh, K., 1984, "Fourier Transform Profilometry for Automatic Measurement of 3D Object Shapes," Appl. Opt., Vol 22, No. 24, pp. 3977~3982.

Yang, I. H., Fujigaki, M., Morimoto, Y. and Han, E. K., 1992, "Strain Analysis of Vibrating Object using Fourier Transform Grid Method," JSNDI(in Japanese), Vol. 41, No. 8, pp. 486~492.

Yang, I. H., 1992, "Analysis of 3D Shape and Strain Distributions of Deformable Object Using Stereo Vision," KSME, Proceedings of the KSME Autumn Annual Meeting, pp. 242~247.